Effects of small-scale gold mining tailings on the underwater light field in the Tapajós River Basin/Brazilian Amazon.

Felipe Lobo[1], Maycira Costa[1], Evlyn Novo[2], Kevin Telmer[3]

1- Spectral Lab, Department of Geography, University of Victoria, 3800 Finnerty Road Victoria, BC, Canada V8P 5C2;
Corresponding author. Phone: (250)472-5223, email: lobo@uvic.ca

2- Remote Sensing Division, National Institute For Space Research (INPE), Av. dos Astronautas 1758, São José dos Campos, SP, Zip code 12227-010, Brazil, Phone: (012) 3208-6447, email: evlyn@dsr.inpe.br

3- Executive Director, Artisanal Gold Council, 101-732 Cormorant St. Victoria, BC, Canada, V8W 4A5. Phone: (250)590-9433, email: ktelmer@artisanalgold.org

1. Introduction

Water siltation caused by gold mining is commonly reported throughout the world (Asia, Africa, and South America) (Mol and Ouboter 2004) because most of the mining activities take place in rivers or at their margins. In the Brazilian Amazon, for example, sediments from mining tailings in streams and rivers may vary between 1 and 2 tonnes per gram of gold produced (Sousa and Veiga 2009). Such practices likely have a remarkable impact on fluvial systems, considering that ASGM (Artisanal and Small Scale Gold Mining) gold production in the Brazilian Amazon reaches an average of 50 tonnes annually (Araújo Neto 2009). One of the effects of water siltation is light attenuation by suspended particles which can directly affect phytoplankton productivity by limiting Photosynthetic Available Radiation (PAR), and indirectly leads to environmental imbalance and biodiversity change in rivers impacted by gold mining (Tudesque et al. 2012). While some evidences show the impacts on underwater light conditions caused by mining tailings (Guenther and Bozelli 2004; Roland and Esteves 1998), the quantification of the impact on the spectral underwater light field in Amazonian waters is still lacking. Understanding the underwater light field, more specifically the total scalar irradiance, *Eo*, is important. Firstly, it informs the total energy available for photosynthesis in a hyperspectral interval between 400 and 700 nm, which in turn allows for spectral analysis on specific phytoplankton absorption efficiency. For example, an underwater light field rich in blue-green light will favour phytoplankton that has pigments that absorb light in the blue-green spectra (Markager and Vincent 2001). Secondly, knowing the total scalar irradiance also allows for the description of bio-optical parameters that can be used in remote sensing approaches to retrieve water quality parameters from satellite images for monitoring purposes (Li et al. 2013; Odermatt et al. 2012; Pahlevan and Schott 2013).

This research focus on defining the impact of gold mining tailings in the light field of Amazonian waters, and associated phytoplankton communities diversity and specific absorption. Specifically, the objectives of this study are: 1) Quantify the optical effects of sediment loading on the underwater light field along non-impacted and impacted rivers in the Tapajós River Basin (Brazilian Amazon); 2) Evaluate to what extent the characteristics of the light field and the light attenuation caused by water siltation impacts the characteristics of the phytoplankton communities and critical depth; 3) Assess the absorption efficiency of two major phytoplankton groups (cyanobacteria and diatom) given the different in situ light conditions observed along the river network.

2. Study Area

The lower section of the Tapajós River Basin covers about 130,370 km^2 (Figure 1) and drains mostly lixiviated Pre-Cambrian rocks, which results in water that is transparent/greenish in color with low amounts of suspended solids, so-called ‘clearwaters’ (Junk et al. 2011). The study area includes the largest small-scale gold mining area in the world (28,186 km^2), which has been intensively mined (Lobo et al. 2016), either using water-jets to remove top soil layers, or using small boats called ‘balsas’ that take the sediment from the bottom of the rivers using suction and gravity processes (Araújo Neto 2009; Telmer et al. 2006). Currently, more than 300 small-scale mines with participation of more than 50,000 miners produce gold within the ‘Reserva Garimperia,’ created in 1983 to support gold miners, and overlapping three main sub-basins: Novo, Crepori, and Tocantinzinho (abbreviated Tocantins) tributaries (see Figure 1 for locations).

3. Methods

To address the objectives, the methodological approach consisted of three major components: 1) Acquisition of in situ optical and biogeochemical data at high (April/2011) and low (Sep/2012) water levels; 2) Calibration and validation of a bio-optical model to derive total scalar irradiance; 3) Evaluation of the critical depth for phytoplankton productivity based on E_o, and assessment of spectral absorption efficiency of two dominant groups, diatom and cyanobacteria, identified in this study.

Biogeochemical and optical data acquisition

Two field campaigns were conducted in the Tapajós River Basin to measure Inherent Optical Properties (IOPs), Apparent Optical Properties (AOPs), and biogeochemical data in March/April 2011 during high water level (27 sample points) and September 2012 during low water level (13 sample points) (see Figure 1 for sample point locations). Locations of the sample points were distributed along the Tapajós River and main tributaries, to cover both mined (Crepori, Tocantins, and Novo) and non-mined tributaries (Jamanxim). Inherent optical properties (IOPs) measurements were only acquired during the high water level campaign (April, 2011, n = 27). Total beam attenuation $c(\lambda)$ and total absorption $a(\lambda)$ coefficients were measured in situ with a WetLabs ac-S instrument at 80 wavelengths from 390 to 750 nm. As reference, IOPs of two non-mined (called pristine) small streams alongside the Crepori River were also sampled. Apparent Optical Properties (AOPs), measures in-water downwelling irradiance ($E_d(0^-, \lambda)$) and upwelling radiance ($L_u(0^-, \lambda)$) were measured using two profiling Satlantic hyperspectral radiometers and one above-water hyperspectral radiometer during both field campaigns (n = 40 Radiometric data were processed using Satlantic's Prosoft (Satlantic 2011).

Bio-optical model to derive scalar irradiance

Given that phytoplankton cells are able to utilize irradiance from all directions, $E_o(0^-,\lambda)$ is required for quantifying light availability for primary production (Kirk 2011).

$$E_o(0^-,\lambda) = E_d\,(0^-,\lambda) + E_u(0^-,\lambda) \qquad (1)$$

where $E_u\,(0^-,\lambda)$ and $E_d\,(0^-,\lambda)$ are upwelling and downwelling scalar irradiance, respectively.

In order to model Eo for both impacted and non-impacted waters Hydrolight was applied. Hydrolight input data used for 40 sample sites were environmental conditions, measured above-water downward irradiance ($E_d\ 0^+,\lambda$), measured IOPs (a_{cdom}, a_p, $b_{p,}$ and volume scattering function-VSF). For those sample points with no IOPs measurements, the mass-specific IOPs derived from in loco measurements were used as alternative to estimate IOPs.

Critical depth for photosynthesis and in situ absorption coefficient

Once the $E_o(0\text{-},400\text{-}700nm)$ was modeled, the critical depth (Z_c) and the absorption efficiency of phytoplankton were estimated for the different groups of water. The critical depth, Z_c, is the depth at which irradiance is the minimum necessary for photosynthesis given a condition of high nutrient availability, and is calculated as follows (Kirk 2011):

$$Z_c\,(PAR) = \frac{ln\,E_o\,(0-,PAR) - ln\,E_c\,(PAR)}{K_o\,(PAR)} \qquad (2)$$

where E_o (0-, PAR) is the sub-surface scalar irradiance modeled by Hydrolight; K_o (PAR) is the average scalar attenuation coefficient for PAR from surface to $Z_{1\%}$ (similar to Equation 7); and E_c (PAR) is the species-specific compensation irradiance. To calculate Z_c in this study, we adopted E_c (PAR) based on the freshwater phytoplankton minimum light requirement described by (Deblois et al. 2013). The authors reported that *Chlamydomonas sp.* (Chlorophyta) (identified in this study) shows a growth rate close to zero when exposed to irradiance of 14 $\mu Em^{-2}s^{-1}$.

The efficiency of the phytoplankton absorption within the PAR spectra is defined based on the in situ specific absorption coefficient of phytoplankton ($in\ situ\ a^*_{ph}(\lambda)$) (Markager and Vincent, 2001). *In situ* specific absorption coefficient depends on the specific phytoplankton absorption coupled with *in situ* light spectrum (Markager and Vincent 2001). It can be calculated as follows (Kishino 1986; Markager and Vincent 2001):

$$in\ situ\ a^*_{ph}(\lambda) = \bar{E_o}(z,\lambda).a^*_{ph}(\lambda) \qquad (3)$$

where $\bar{E}_o(z,\lambda)$ represents modeled E_o (z,λ) normalized to measured $E_d(0^+, \lambda)$, and $a^*_{ph}(\lambda)$ is the phytoplankton specific absorption coefficient. The specific absorption (a^*_{ph}) of two phytoplankton species reported by (Bricaud et al. 1988) were used in this study: a cyanobacteria (*Synechocystis sp.*), which is a freshwater species identified in this study, and a diatom (*Chaetoceros sp.*), found in the oceans.

4. Results and Discussion

The biogeochemical data was stratified into five preliminary classes according to the intensity of water siltation, aiming to facilitate the interpretation of the results (Figure 2).

Spatial and temporal TSS distribution

From this dataset, the TSS (Total Suspended Solids) concentrations in the mined rivers varies spatially and seasonally as a result of the annual dynamics of the flood pulse (Junk 1997; Melack and Forsberg 2001), the biogeochemistry and geology of the watershed (Junk, 2013), and the gold mining activities (Lobo et al. 2015; Telmer and Stapper 2007).

In the upstream area (see Figure 1), despite of a few mining operations, the measured sediment concentration is very low, resulting in a relatively deep euphotic zone (~ 5.5 m). In these waters, the suspended sediment has a considerable amount of organic matter (~ 30 % of TSS), composed mostly of allochthonous plant debris (Roulet et al., 1998; Bernardes et al., 2004). The characteristics and concentration of the suspended sediments change abruptly as the Tapajós River receives clay-rich tributaries, such as the heavily-mined Crepori River (TSS~111.3 $mg.L^{-1}$ and organic matter < 3%, euphotic depth ~ 2.0 m). Similarly, TSS at the Jamanxim River increases (*Class 1* and *Class 2*) as it receives sediment-rich discharge from the Novo and the Tocantins sub-basins (Figure 2) subject to mining operations. The sediment plume from the Crepori River only fully mixes with the Tapajós River waters after receiving the Jamanxim River discharge and passing through rapids (Figure 1) about 200 km downstream (Lobo et al. 2015; Telmer et al. 2006). After the rapids, as the sediment load dilutes and the water velocity decreases, the suspended solids sink and TSS concentration decreases to values similar to those of the upstream Tapajós River.

Seasonally, the increase of TSS from ebbing to rising water periods is in part a result of the suspended solids input carried during rain events as the water rises (Junk 1997; Melack and Forsberg 2001). Gold mining activities are also temporally dynamic, that is, during the rainy

season most of the gold mining activity discontinues (Bezerra et al. 1998), and dilution due to an increase in volume of water in the rivers causes the sediment concentration to decrease. When the rainy season ends, mining activities intensify, and together with the lower water volume in the dry season, increased concentrations of sediment to levels above 100 $mg.L^{-1}$ are typical (Figure 2).

Phytoplankton and pigments

The phytoplankton microscopy analysis indicated some general tendencies. First, a higher biovolume (mm3.L-1) was measured during the low water period compared to the high water period. However, due to sampling constraints, a direct seasonal comparison was only possible for the Crepori and Tapajós_Itaituba sites, which both indicated lower productivity during the high water compared to the lower water period (Figure 3). Second, changes were observed in the phytoplankton community from upstream tributaries, where the phytoplankton biovolume was lower (value) and with dominance of diatoms and cryptomonads when compared to the Tapajós Lake section where most of the phytoplankton biovolume was higher (value) and dominated by cyanobacteria cells.

Optical changes

Sediment flushed into the rivers from small-scale mining operations is composed of an agglomeration of fine clay particles (Telmer et al. 2006; Veiga 1997), mostly kaolinite (Cprm 2009). These mine-derived clay particles cause general changes in magnitude and spectral dependency of IOPs and AOPs compared with water under less or no influence of mined rivers (Figures 4). This is mostly because fine inorganic clay particles tend to be more effective at scattering light due to their lower specific absorption coefficient and higher refractive indexes compared to large inorganic particulates (silt, medium sand), organic particulates such as *flocs* (agglomeration of particles), and phytoplankton (Binding et al. 2005; Bowers and Binding 2006). In waters with increased TSS loadings from mining operations, the scattering coefficient increases, thus resulting in a *b:a* increase for *Class 4* from 7.0 to 100.0 at the blue and red spectra, respectively. In this case, the scattering process prevails over absorption specifically at the green and red wavelengths, thus explaining the observed higher underwater light availability at the green and, mainly, at the red wavelengths (Figure 4). In turbid waters where the *b:a* in the blue spectra is approximately 30.0, such as the case for *Class 4*, $E_{o(0.3m)}$ values became 50% higher than $E_{d(0+)}$ (Figure 4). As the scattering coefficient increases relative to the absorption coefficient, the underwater light becomes more diffuse, thus constraining light to shallower depths in comparison to non-impacted waters. The optical data also indicated that light attenuation was wavelength dependent and higher at blue wavelengths. The remaining underwater available light for both impacted and non-impacted waters was mostly at green and red wavelengths (Figure 4c).

Both scattering and backscattering coefficients are primarily controlled by mineral concentration (TSS), as reported by several authors (Bergmann 2004; Boss and Pegau 2001; Doxaran et al. 2012; Lorthiois et al. 2012; Stramski et al. 2004; Sun et al. 2009). Increasing TSS concentration yielded positive and significant ($p < 0.05$) correlation with $b_{p(660nm)}$, $b_{bp(660)}$, and $a_{p(440)}$. Correlations of optical properties with *chl-a* and $a_{cdom(440)}$ were not significant (correlations not shown), which is explained by the inorganic nature of the soils subject to mining in the Tapajós watershed (Cprm 2009; Rodrigues et al. 1994).

Absorption by dissolved organic matter, $a_{cdom440}$, showed low variability among the defined water classes (~2.6 ± 0.6 m^{-1}), but its contribution to total absorption (a_{440}) is inversely correlated to TSS; it decreases from 60% in pristine streams to 40% in the Tapajós Lake, and 8% for *Class 4*

(the Crepori River), for example. The modeled absorption coefficient by algal particles (a_{ph}) showed low contribution to the total absorption at 440 nm with values not higher than 3% for both mined and non-impacted rivers. This is similar to data reported for streams impacted by gold mining tailings in New Zealand, where TSS discharge is also the prevailing factor attenuating incoming light (Davies-Colley et al. 1992).

Critical depth and in situ specific absorption for phytoplankton

The light compensation depth or critical depth, Z_c, for *Chlamydomonas sp* indicated that in pristine streams enough light was available for photosynthesis up to 7.0 m depth. The critical depth decreased to ~5.2 m for *Class 1* waters. As water turbidity increased a decrease in Z_c was observed, thus resulting in a critical depth of 4.0, 3.7, 2.4, and 1.6 m for *Class 2*, *Class 3*, *Class 4*, and, *Class 5*, respectively.

The estimated *in situ* specific absorption (in situ a^*_{ph}) for the representative phytoplankton groups, diatom and cyanobacteria, showed slightly higher absorption in the blue region of the spectra for diatoms; overall, cyanobacteria are generally more efficient at absorbing PAR than diatoms due to absorption peak at 622 nm. For example, at the sub-surface of pristine rivers, the in situ $a^*_{ph\ (PAR,\ diatom)}$ was 0.62 $m^{-2}.mg^{-1}$, whereas for cyanobacteria it was 0.70 $m^{-2}.mg^{-1}$. For *Class 4*, at sub-surface, the in situ $a^*_{ph\ (PAR,\ diatom)}$ (0.61 $m^{-2}.mg^{-1}$) was similar to that of pristine streams (0.62 $m^{-2}.mg^{-1}$) due to very high absorption at 675 nm. However, for *Class 5*, the reduction of in situ a^*_{ph} at the blue spectra was no longer compensated by the very high absorption in the red spectra (in situ $a^*_{ph\ (PAR,\ diatom)}$ = 0.48 $m^{-2}.mg^{-1}$). At 2.0 m depth, the in situ $a^*_{ph\ (PAR,\ diatom)}$, for example, decreased from 0.11 $m^{-2}.mg^{-1}$ in pristine rivers to values close to 0.01 $m^{-2}.mg^{-1}$ in turbid waters due to the low light availability.

Analysis of in situ specific absorption coefficient (a^*_{ph}) for two major phytoplankton groups (cyanobacteria and diatoms) suggested that the absorption system of cyanobacteria would be more efficient than that of diatoms given an underwater environment dominated by red wavelengths. Since no difference of phytoplankton biovolume and pigments among impacted and non-impacted rivers was observed (Figure 3), the results indicated that other physical/chemical factors, such as the interaction between critical and mixed layer depth, current velocity, and nutrient concentrations could also play an important role in controlling phytoplankton productivity and diversity in the rivers subjected to mine tailings impact.

For example, in fast flowing waters with current speeds of approximately 0.5 $m.s^{-1}$ during the high water period, such as the study waters (impacted, non-impacted, and upstream Tapajós), the turbulence and high flushing rates prevent phytoplankton growth. In terms of planktonic group, even if at low concentration levels, diatoms are prevailing (*Tabelaria sp., Aulacosera granulate, and Urosolenia eriensis*) in these fast flowing waters (Figure 7). The presence of siliceous exoskeleton increases diatom survival in high water flow rivers (Huisman et al. 2004). The dominance of diatoms is an indicator that water velocity is also an important factor controlling phytoplankton growth and assemblage in these rivers, which is in agreement with other studies in the Amazon Basin (Junk 1997; Kruk et al. 2010). At the Tapajós main channel, where the river is wider than the tributaries, the presence of 'dead zones' (reduced water flow) at the margins (Tockner et al. 2000) allows for higher phytoplankton production (> 1.0 $\mu g.L^{-1}$) when compared to the upstream tributaries (Table 1).

5. Conclusions

This paper investigated the effects of water siltation on the underwater light field of different tributaries of the Tapajós River Basin, and its consequences to the phytoplankton community to fill the gap of knowledge related to ASGM impacts on water quality. The effects of introduced TSS derived from mining activities on both the inherent and apparent optical properties were quantified and E_o modeled using Hydrolight. Results showed that the inorganic nature of mine tailings is the main factor affecting the underwater scalar irradiance in the Tapajós River Basin. The TSS concentration varies seasonally during the year in a synergism between water level and mining activities: during low water level, mining activities intensify and, associated with low water volume, TSS rapidly increases, which in turn changes the optical characteristics of the water. For waters with low or no influence from mine tailings, light absorption dominates over scattering. With increased TSS loadings from mining operations, the scattering process prevails over absorption coefficient, and, at sub-surface, scalar irradiance is reduced, resulting in a shallower euphotic zone, and green and red wavelengths dominate.

Although a strong light reduction due to water siltation was observed in impacted tributaries, the effects on the phytoplankton community was not clearly observed, which can be attributed to: i) low number of samples for proper comparison between impacted and non-impacted tributaries; and ii) general low phytoplankton productivity in all upstream tributaries due to a combination of high current velocity (flushing), and variable availability of nutrient and light conditions.

Secondly, we consider the efficiency of two phytoplankton groups to absorb available spectral light over the PAR range. Based on our in situ data and literature review, we demonstrate that cyanobacteria (*Synechocystis sp*.) could be more efficient at absorbing the spectral available light in both impacted and non-impacted waters in comparison to diatoms (*Chaetoceros sp.*). Given the high dominance of red wavelength in the modeled underwater light field, the higher efficiency of the cyanobacteria can be attributed to the presence of auxiliary pigments such as phycocyanin (with a peak of absorption centered at 620 nm). However, the dominance of diatoms in the tributaries suggests that the spatial and temporal distribution of phytoplankton in the Tapajós River Basin is not simply a function of light availability, but rather depends on a synergism of factors including flood pulse, water velocity, seasonal variation of incoming irradiance, and nutrient availability.

Acknowledgements

This research was developed in a partnership between the University of Victoria (UVic), the Brazilian Institute for Space Research (INPE), and the Artisanal Gold Council. The authors would like to acknowledge logistical support by ICMBio (Brazilian Agency of Protected Areas) represented by MSc. Haroldo Marques. We also acknowledge financial support from the National Sciences and Engineering Research Council of Canada (NSERC) to Dr. Costa, from FAPESP (Process 2011/23594-8) to Dr. Novo, and from *Science Without Borders - Brazilian Program* (237930/2012-9), which supported the lead author as part of his PhD research project.

References

Araújo Neto, H. 2009. Perfil do Ouro. Ministério de Minas e Energia.

Bergmann, T. 2004. Impacts of a recurrent resuspension event and variable phytoplankton community composition on remote sensing reflectance. Journal of Geophysical Research **109**.

Bezerra, O., A. Veríssimo, and C. Uhl. 1998. Impactos da garimpagem de ouro na Amazônia Oriental. Imazon.

Binding, C. E., D. G. Bowers, and E. G. Mitchelson-Jacob. 2005. Estimating suspended sediment concentrations from ocean colour measurements in moderately turbid waters; the impact of variable particle scattering properties. Remote Sensing of Environment **94:** 373-383.

Boss, E., and W. S. Pegau. 2001. Relationship of light scattering at an angle in the backward direction to the backscattering coefficient. Applied Optics **40:** 5503-5507.

Bowers, D. G., and C. E. Binding. 2006. The optical properties of mineral suspended particles: A review and synthesis. Estuarine Coastal and Shelf Science **67:** 219-230.

Bricaud, A., A.-L. Bédhomme, and A. Morel. 1988. Optical properties of diverse phytoplanktonic species: experimental results and theoretical interpretation. Journal of Plankton Research **10:** 851-873.

Cprm. 2009. Província mineral do Tapajós: geologia, metalogenia e mapa previsional para ouro em SIG. http://www.cprm.gov.br accessed in April, 2013.

Davies-Colley, R., C. Hickey, J. Quinn, and P. Ryan. 1992. Effects of clay discharges on streams. Hydrobiologia **248:** 215-234.

Deblois, C. P., A. Marchand, and P. Juneau. 2013. Comparison of Photoacclimation in Twelve Freshwater Photoautotrophs (Chlorophyte, Bacillaryophyte, Cryptophyte and Cyanophyte) Isolated from a Natural Community. PLoS ONE **8:** e57139.

Doxaran, D., J. Ehn, S. Bélanger, A. Matsuoka, S. Hooker, and M. Babin. 2012. Optical characterisation of suspended particles in the Mackenzie River plume (Canadian Arctic Ocean) and implications for ocean colour remote sensing. Biogeosciences **9:** 3213-3229.

Guenther, M., and R. Bozelli. 2004. Effects of inorganic turbidity on the phytoplankton of an Amazonian Lake impacted by bauxite tailings. Hydrobiologia **511:** 151-159.

Huisman, J. and others 2004. Changes in turbulent mixing shift competition for light between phytoplankton species. Ecology **85:** 2960-2970.

Inpe. 2011. PRODES Project. www.obt.inpe.br/prodes accessed in Jun, 2011.

Junk, W. 1997. General Aspects of Floodplain Ecology with Special Reference to Amazonian Floodplains, p. 3-20. *In* W. Junk [ed.], The Central Amazon Floodplain. Ecological Studies. Springer Berlin Heidelberg.

Junk, W. J., M. T. F. Piedade, J. Schöngart, M. Cohn-Haft, J. M. Adeney, and F. Wittmann. 2011. A Classification of Major Naturally-Occurring Amazonian Lowland Wetlands. Wetlands **31:** 623-640.

Kirk, J. T. O. 2011. Light and photosynthesis in aquatic ecosystems. Cambridge University Press.

Kishino, M. 1986. Light utilization efficiency and quantum yield of phytoplankton in a thermally stratified sea. Limnology and oceanography **31:** 557-566.

Kruk, C. and others 2010. A morphological classification capturing functional variation in phytoplankton. Freshwater Biology **55:** 614-627.

Li, L. and others 2013. An inversion model for deriving inherent optical properties of inland waters: Establishment, validation and application. Remote Sensing of Environment **135:** 150-166.

Lobo, F., M. Costa, E. Novo, and K. Telmer. 2016. Distribution of Artisanal and Small-Scale Gold Mining in the Tapajós River Basin (Brazilian Amazon) over the Past 40 Years and Relationship with Water Siltation. Remote Sensing **8 (7):** 22.

Lobo, F. L., M. P. F. Costa, and E. M. Novo. 2015. Time-series analysis of Landsat-MSS/TM/OLI images over Amazonian waters impacted by gold mining activities. Remote sensing of environment **157:** 170-184.

Lorthiois, T., D. Doxaran, and M. Chami. 2012. Daily and seasonal dynamics of suspended particles in the Rhône River plume based on remote sensing and field optical measurements. Geo-Marine Letters **32:** 89-101.

Markager, S., and W. F. Vincent. 2001. Light absorption by phytoplankton: development of a matching parameter for algal photosynthesis under different spectral regimes. Journal of Plankton Research **23:** 1373-1384.

Melack, J., and B. Forsberg. 2001. Biogeochemistry of Amazon floodplain lakes and associated wetlands. The biogeochemistry of the Amazon basin and its role in a changing world**:** 235-276.

Mol, J. H., and P. E. Ouboter. 2004. Downstream effects of erosion from small-scale gold mining on the instream habitat and fish community of a small neotropical rainforest stream. Conservation Biology **18:** 201-214.

Odermatt, D., A. Gitelson, V. E. Brando, and M. Schaepman. 2012. Review of constituent retrieval in optically deep and complex waters from satellite imagery. Remote Sensing of Environment **118:** 116-126.

Pahlevan, N., and J. R. Schott. 2013. Leveraging EO-1 to Evaluate Capability of New Generation of Landsat Sensors for Coastal/Inland Water Studies. Selected Topics in Applied Earth Observations and Remote Sensing, IEEE Journal of **6:** 360-374.

Rodrigues, R. M., A. F. S. Mascarenhas, A. H. Ichihara, and T. M. C. Souza. 1994. Estudo dos impactos ambientais decorrentes do extrativismo mineral e poluição mercurial no Tapajós - Pré-Diagnóstico. CETEM/CNPq.

Roland, F., and F. D. Esteves. 1998. Effects of bauxite tailing on PAR attenuation in an Amazonian crystalline water lake. Hydrobiologia **377:** 1-7.

Satlantic. 2011. ProSoft 7.7 User Manual. *In* http://satlantic.com/sites/default/files/documents/ProSoft-7.7-%20Manual.pdf [ed.], SAT-DN-00228. Satlantic Inc.

Sousa, R. N., and M. M. Veiga. 2009. Using Performance Indicators to Evaluate an Environmental Education Program in Artisanal Gold Mining Communities in the Brazilian Amazon. Ambio **38:** 40-46.

Stramski, D., E. Boss, D. Bogucki, and K. J. Voss. 2004. The role of seawater constituents in light backscattering in the ocean. Progress in Oceanography **61:** 27-56.

Sun, D. and others 2009. Light scattering properties and their relation to the biogeochemical composition of turbid productive waters: a case study of Lake Taihu. Applied Optics **48:** 1979-1989.

Telmer, K., M. Costa, R. Simões Angélica, E. S. Araujo, and Y. Maurice. 2006. The source and fate of sediment and mercury in the Tapajós River, Pará, Brazilian Amazon: Ground- and space-based evidence. Journal of environmental management **81:** 101-113.

Telmer, K., and D. Stapper. 2007. Evaluating and Monitoring Small Scale Gold Mining and Mercury Use: Building a Knowledge-base with Satellite Imagery and Field Work.

Tockner, K., F. Malard, and J. V. Ward. 2000. An extension of the flood pulse concept. Hydrological Processes **14:** 2861-2883.

Tudesque, L., G. Grenouillet, M. Gevrey, K. Khazraie, and S. Brosse. 2012. Influence of small-scale gold mining on French Guiana streams: Are diatom assemblages valid disturbance sensors? Ecological Indicators **14:** 100-106.

Veiga, M. M. 1997. Mercury in Artisanal Gold Mining in Latin America: Facts, Fantasies and Solutions. UNIDO.

FIGURES AND TABLES

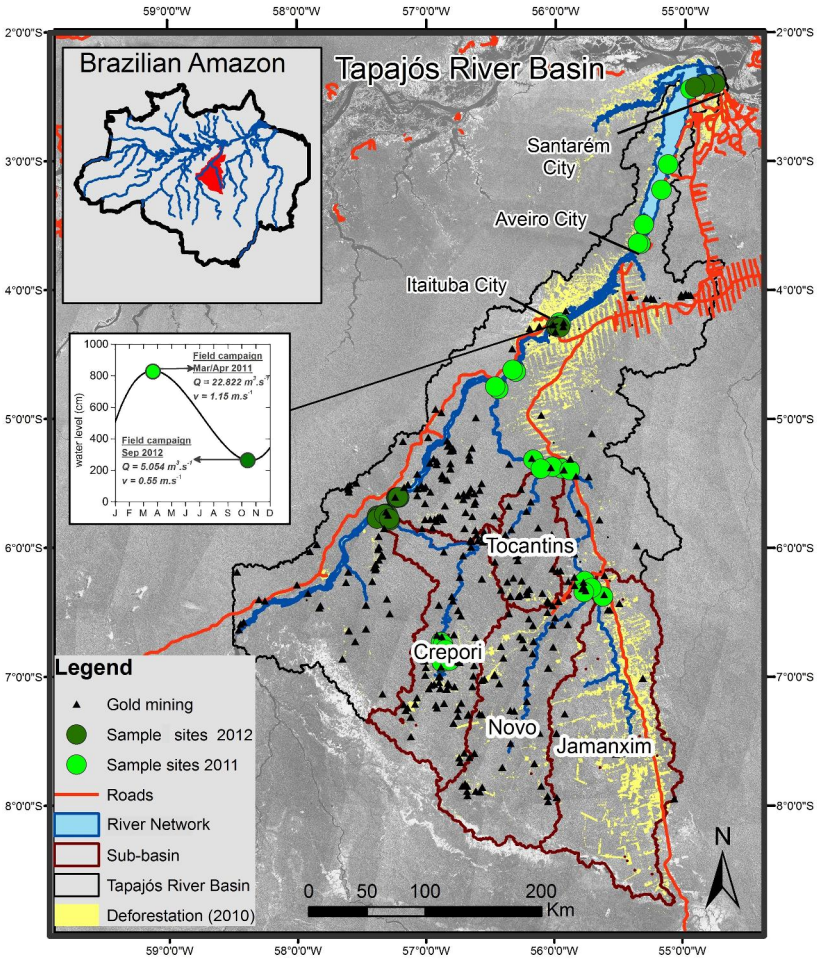

Figure 1: Location of the Tapajós River Basin in the Brazilian Amazon showing the main cities, main tributaries, sample sites (see section 4.1), deforestation (Inpe 2011), gold-mining district, and mines (Cprm 2009). Water flow (Q) and water speed (v) are also shown for the Itaituba City region during high and low water level.

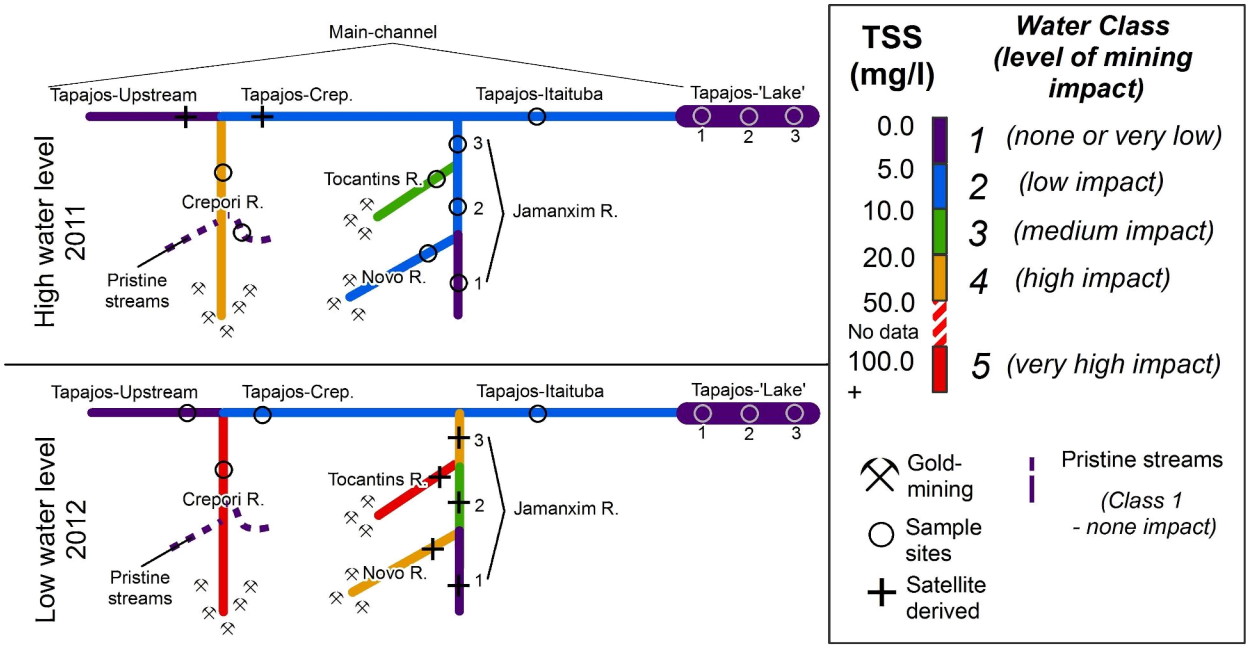

Figure 2: Schematic representation of TSS (Total Suspended Solids) concentrations along the Tapajós River and its tributaries for high (April 2011) and low (September 2012) water levels. The river and its tributaries were classified according to TSS (mg.L^{-1}) concentrations. TSS for Tocantins, Novo, and Jamanxim rivers during the low water season were retrieved from Landsat $\rho_{surf}\ (red)$, surface reflectance (Lobo et al. 2015). Numbers represent location from upriver (1) to downriver (3) on the Jamanxim River and Tapajós 'Lake' section (figure not to scale). Level of mining impact is an arbitrary classification (*Classes* 1 to 5) considering the mining area distribution.

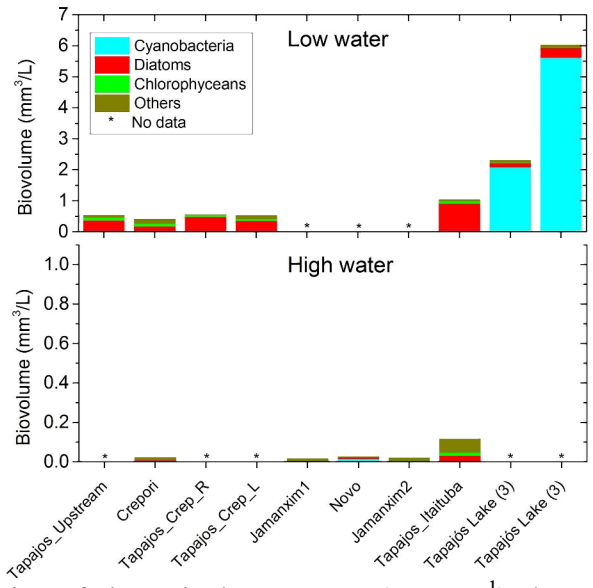

Figure 3: Spatial distribution of phytoplankton groups (mm3.L^{-1}) along the Tapajós River for high and low water level periods.

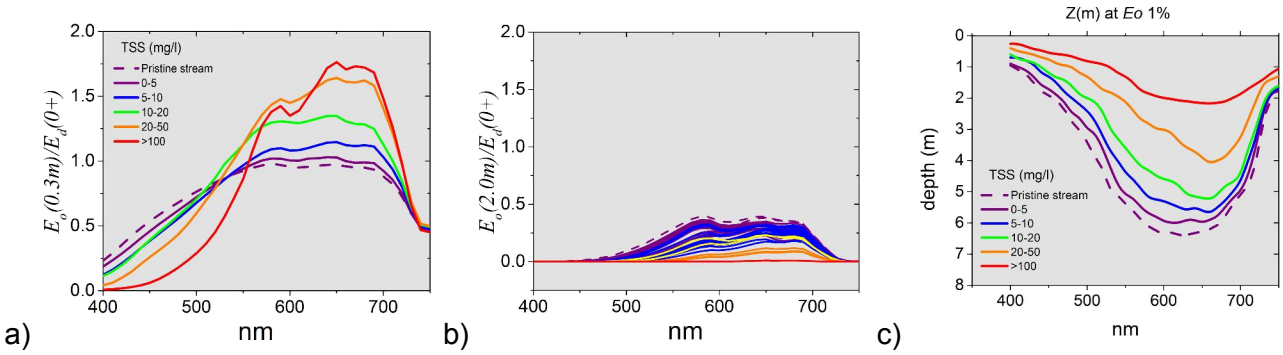

Figure 4: Normalized scalar irradiance at 0.3 m (a) and at 2.0 m deep (b) for all samples grouped by TSS. c) Spectral profile of $Z_{1\%}$ averaged for each class.

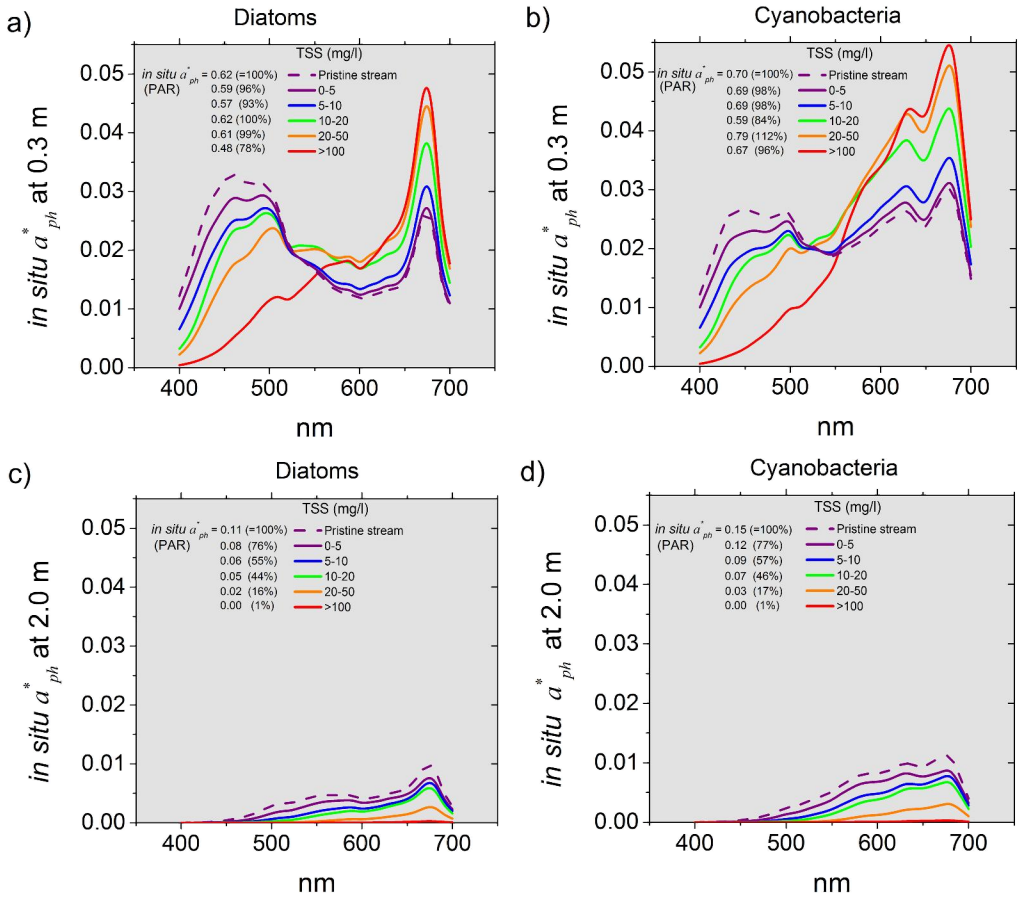

Figure 5: Spectral distribution of in situ $a^*_{ph\ (\lambda)}$ by diatom and cyanobacteria given the normalized E_o at sub-surface (0.3 m, a-b) and at 2.0 m deep (c-d). The integral of in situ $a^*_{ph\ (PAR)}$ for all curves are shown in the corresponding graph with relative percentage (%) based on pristine streams (taken as 100%).

Table 1: Schematic representation of the main factors controlling phytoplankton group and productivity (*chl-a* and biovolume) from upstream tributaries to mouth.

	Tributaries		**Tapajós - Itaituba (Main channel)**	**Tapajós-Lake**
	not mined	**mined**		
Z_m/Z_c	~1.1	~ 2.0	~1.2	~ 0.4
Light availability	not limiting	reduced and possibly limiting	not limiting	Not limiting. Possibly, at deep mixed layers (>8m)
Nutrients	oligotrophic	eutrophic	oligo/meso	oligotrophic
chl-a	Low (<1.0 $\mu g.L^{-1}$)	Low (<1.0 $\mu g.L^{-1}$)	Med (<2.0 $\mu g.L^{-1}$)	Med/high (<10.0 $\mu g.L^{-1}$)
Taxon	diatoms	diatoms	diatoms/chrypto	cyanobacteria
Flushing (water velocity)	high (0.2 to 1 $m.s^{-1}$)	high (0.2 to 1 $m.s^{-1}$)	high with 'dead zones' (0.4 to 1.3 $m.s^{-1}$)	low/med, allows buoyancy